

4D Cryo-Electron Microscopy of Proteins

Anthony W. P. Fitzpatrick, Ulrich J. Lorenz, Giovanni M. Vanacore, and Ahmed H. Zewail*

Physical Biology Center for Ultrafast Science and Technology, Arthur Amos Noyes Laboratory of Chemical Physics, California Institute of Technology, Pasadena, California, 91125 United States.

S Supporting Information

ABSTRACT: Cryo-electron microscopy is a form of transmission electron microscopy that has been used to determine the 3D structure of biological specimens in the hydrated state and with high resolution. We report the development of 4D cryo-electron microscopy by integrating the fourth dimension, time, into this powerful technique. From time-resolved diffraction of amyloid fibrils in a thin layer of vitrified water at cryogenic temperatures, we were able to detect picometer movements of protein molecules on a nanosecond time scale. Potential future applications of 4D cryo-electron microscopy are numerous, and some are discussed here.

Structural biology is entering a new and exciting age. It is clear that the structure–function paradigm is insufficient to fully establish the molecular mechanisms of many biological processes and that the integration of the fourth dimension, time, into structural biology methods is fundamental to our understanding of the relationship between structure, dynamics, and function.¹ Four-dimensional electron microscopy² (4D EM) has recently been extended to the realm of biological structures, making possible imaging of the motion of DNA networks³ and amyloid-like microcrystals.⁴ However, 4D EM of biological specimens under native-like conditions has not been realized. It has been proposed that 4D cryo-electron microscopy (4D cryo-EM), in which a protein molecule is embedded in glassy ice, would permit the visualization of the ultrafast dynamics of biomolecules in a fully hydrated state,⁵ but to date imaging of the motions involved has not been reported.

In this communication, we present a proof-of-principle set of experiments showing that it is possible to obtain 4D cryo-EM images and diffraction patterns of a network of insulin amyloid fibrils, a prototypical biomacromolecule,⁶ in a time-resolved manner and directly visualize the movements of the constituent protein molecules. The length and time scale involved are picometer and nanosecond, respectively.

The concept of the experiment is as follows: the high spatiotemporal resolution of 4D EM is used to visualize the dynamics of a thin film of photoresponsive amyloid fibrils embedded in vitreous ice (Figure 1). A precisely timed laser (pump) pulse and electron (probe) pulse are used, respectively, to heat/excite and image/diffract the sample using different delay times, thus generating a series of “frames” at discrete time points (Figure 1). This time series of frames directly shows the structural dynamics of the fibrils in the environment of living organisms, i.e. hydrated.⁷

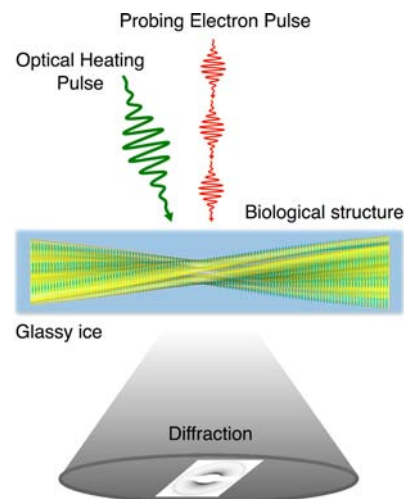


Figure 1. Four-dimensional cryo-electron microscopy of biological specimens. A biological specimen, here we use amyloid fibrils shown in yellow, is embedded in glassy ice and heated using a (pump) laser pulse. A timed (probe) electron pulse is used to image/diffract the hydrated sample at different delay times. The induced movements in the protein assembly can be determined from changes in the time-resolved diffraction patterns. The representative amyloid fibril image was created using PDB ID 2m5m and EMDB ID EMD-2323.⁸

Amyloid fibrils have a characteristic “cross- β ” structure composed of paired hydrogen-bonded β -sheets running parallel to the long axis of the fibrils.⁸ The regular interstrand spacing results in a distinctive 0.48 nm cross- β reflection in X-ray⁹ and electron fiber diffraction¹⁰ (Figure 2). By triggering an expansion of the cross- β interface using a temperature jump, we can accurately determine the stretching of the β -sheets (Figure 3) by monitoring the change in radius of the 0.48 nm fiber diffraction rings.

Many proteins are poor absorbers of visible light, and so to efficiently transfer heat into the fibrils, we bind a small amyloidophilic dye molecule, Congo red, to the outer surface of the fibrils.¹¹ Note that the Congo red molecule does not perturb the cross- β structure and that by exciting the dye directly, energy is transferred to the fibrils within the vitreous ice.

To begin, we performed T-jump experiments on the amyloid fibrils deposited on lacey carbon grids using the stroboscopic mode of our 4D EM at room temperature (Figure 2a, b). Firing nanosecond ultraviolet pulses (4.66 eV, 2.8 μ J/pulse, 10 ns

Received: November 11, 2013

Published: December 6, 2013

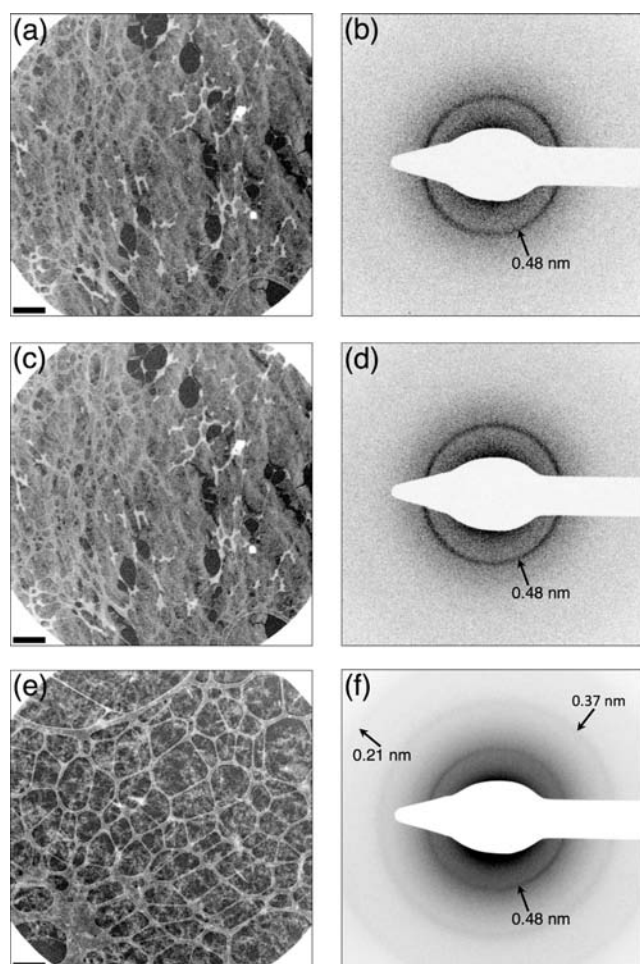


Figure 2. Images and selected area diffraction patterns of a network of amyloid fibrils taken using our 4D cryo-electron microscope. Protein density is shown in white on a lacey carbon substrate. A magnified view of the sample is shown in Figure S1 in Supporting Information. (a) Image and (b) diffraction pattern of a network of amyloid fibrils taken at room temperature (300 K). Note the strong 0.48 nm reflection, a hallmark of amyloid structure, corresponding to the interstrand separation within β -sheets. (c) Image and (d) diffraction pattern of the same area in (a and b, respectively) acquired at cryogenic temperatures (118 K, in the absence of vitreous ice) showing no change in the morphology of the fibril network or the 0.48 nm ring. (e) Image and (f) diffraction pattern of fibrils embedded in vitreous ice taken at 118 K. In addition to the characteristic 0.48 nm amyloid ring; note the defining reflections indicating the presence of vitreous ice: a strong broad ring at 0.37 nm and a weaker ring at 0.21 nm. The scale bar in real-space images (a, c, e) corresponds to a distance of 2 μm .

fwhm, 25 ns jitter) at the LaB₆ source to generate probe photoelectron packets, and using a (green) pump fluence of ~ 6 mJ/cm² at a 1 kHz repetition rate, we collected a series of fiber diffraction frames using delay times ranging from -100 to 500 ns in 50 ns increments. As expected, before time zero, there are no dynamics (Figure 3a). There is then an immediate expansion of the fibrils (Figure 3a) as the laser pulse heats the sample, by ~ 2 K (see Supporting Information [SI] and Figure S2), resulting in a decreased radius of the interstrand reflection (in reciprocal space, Figure 2b). At room temperature, this relative expansion $\Delta x/x_e$, where Δx is the expansion and x_e is the equilibrium separation (i.e., 0.48 nm), is $4.0 \pm 0.2 \times 10^{-3}$ (Figure 3a) corresponding to 1.9 ± 0.1 pm (Figure 3b).

Since the fibril heating is uniform and homogeneous, the expansion along the long axis of the fibril can be considered to be a stretching of $\Delta x/2 = 1$ pm ($1.9/2$ pm) in opposite directions (Figure 3b). It is important to note that these dynamics do not arise from expansion of the lacey carbon substrate, as control experiments were performed on both silicon nitride and bare copper grids, and the dynamics were identical.

Next, using a temperature-controlled cryo-holder, we lowered the temperature of the fibrils to 118 K via liquid nitrogen cooling of the specimen holder. In this way, a T-jump experiment (using the same pump fluence as before) was performed to investigate the fibril dynamics at liquid nitrogen temperatures in the absence of vitreous ice (Figure 2c,d). Interestingly, we found an increased expansion of the hydrogen-bonded β -sheets (Figure 3c, d) compared to our room temperature experiments, namely, $7.4 \pm 0.3 \times 10^{-3}$ corresponding to a total expansion of 3.5 ± 0.1 pm (or $3.5/2 = 1.8$ pm in opposite directions, Figure 3d). This may be due to an increased absorption cross section of the dye at low temperatures,¹² or it may reflect a decrease in the heat capacity of the fibrils at low temperatures¹³ via:

$$f = \int_{T_e}^{T_e + \Delta T} C_p dT$$

where f and C_p are the absorbed energy per unit volume and heat capacity of the material, respectively, T is temperature with T_e being the equilibrium temperature and ΔT the temperature jump. Since the pump fluence is unchanged from the room temperature experiments, either the absorbed energy has increased due to enhanced absorption of the Congo red dye at low temperatures, or the heat capacity of the fibrils has decreased in the colder environment. Either way, the temperature jump must have been doubled at 118 K to give rise to twice the fibril expansion relative to that measured at room temperature (Figure 3a–d).

Finally, we measured the dynamics of fibrils embedded in unsupported vitreous ice at 118 K. Despite the strong attenuation of the (photo) electron beam by the vitreous ice, the fibril ring at 0.48 nm is still clearly visible (Figure 2e,f). Note also the presence of the characteristic diffraction rings from vitreous ice⁷ with a strong, broad ring at 0.37 nm and a weaker ring at 0.21 nm indicating that the fibrils are in the aqueous environment (Figure 2f).

Using the same pump fluence as before (~ 6 mJ/cm²), we again saw an increased expansion of the hydrogen-bonded β -sheets upon initiation of the laser-induced T-jump with a relative expansion of $11.3 \pm 1.2 \times 10^{-3}$ (Figure 3e) corresponding to a movement of 5.4 ± 0.6 pm (or $5.4/2 = 2.7$ pm in opposite directions, Figure 3f). This increased expansion by almost a factor of 2 compared to that measured at 118 K in the absence of glassy ice can be rationalized by considering that amyloid fibrils are mainly stabilized by a network of interbackbone hydrogen bonds^{8,14} (Figure 3b,d,f). From experiment^{15–17} and computation,¹⁸ the strength of a hydrogen bond in vacuum is ~ 4.8 kcal/mol which is reduced to ~ 1.5 kcal/mol in the presence of water. Therefore, we interpret the increased expansion of the β -sheets following the T-jump (Figure 3e) as a reflection of the weakening of the fibrils' hydrogen-bonding network in the aqueous environment (Figure 3f) making the fibrils more stretchable.

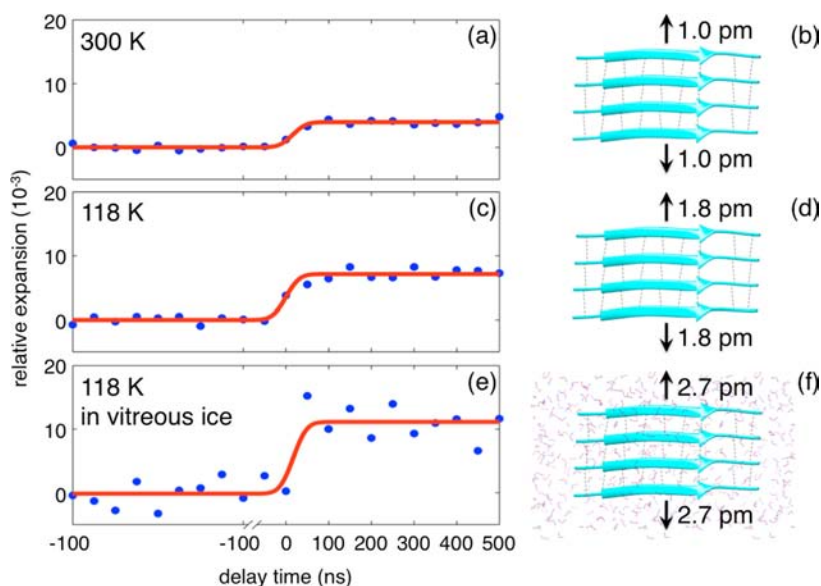


Figure 3. Protein dynamics measured using 4D cryo-EM. The left half of the figure (a, c, e) shows plots of the relative expansion of the amyloid fibrils as a function of time. The right-hand side shows schematics of the expansion of the fibrils' constituent β -sheets in picometers. Individual β -strands, connected by interbackbone hydrogen bonds (black dashed lines), are shown as cyan ribbons. The fluence of the pump pulse in all cases is ~ 6 mJ/cm². It is important to note that 10 data points were acquired before time zero to ensure that there were no dynamics prior to the T-jump. (a) Room temperature fibril dynamics revealed a stretching of the (b) hydrogen-bonded β -sheets by 2 pm, or 1 pm in opposite directions, along the long axis of the fibril. (c) At cryogenic temperatures in the absence of vitreous ice, there is an increased expansion of the β -sheets (d) of 3.5 pm, or 1.8 pm in opposite directions. (e) When the fibrils are hydrated in vitreous water and kept cool at 118 K, there is an increased expansion of the fibril in response to the T-jump. This is shown schematically in (f) as a hydrated β -sheet with water molecules displayed as red and blue V-shaped lines (oxygen and hydrogen atoms are shown in red and blue, respectively). The absolute expansion under these conditions is 5.4 pm, or 2.7 pm in opposite directions. The representative β -sheet image was created using PDB ID 2m5n.⁸

In conclusion, we have shown that the development of 4D cryo-EM enables the detection of picometer-scale movements occurring in hydrated proteins on a nanosecond time scale. This proof-of-principle experiment paves the way for ultrafast structural dynamics studies of 2D membrane protein crystals¹⁹ and 3D micro- or nanocrystals²⁰ embedded in vitreous ice. Indeed, the conformational changes in biologically active protein crystals are often much larger than the ~ 5 pm movement we have detected here, and many of these movements occur on the nanosecond, or faster, time scales.²¹ It is for these reasons that we expect that 4D cryo-EM will have wide-ranging applications in the exciting field of dynamical biology.

■ ASSOCIATED CONTENT

Supporting Information

Materials and methods, a close-up view of the amyloid fibril network (Figure S1) and calibration of the laser-induced temperature jump via temperature-controlled static diffraction (Figure S2). This material is available free of charge via the Internet at <http://pubs.acs.org>.

■ AUTHOR INFORMATION

Corresponding Author

zewail@caltech.edu

Notes

The authors declare no competing financial interest.

■ ACKNOWLEDGMENTS

This work was supported by the National Science Foundation and the Air Force Office of Scientific Research in the Physical Biology Center for Ultrafast Science and Technology (UST)

supported by the Gordon and Betty Moore Foundation at Caltech. A.W.P.F. is supported by a Marie Curie International Outgoing Fellowship. We thank A. W. McDowell and the Beckman Institute for help with sample preparations and for useful discussions.

■ REFERENCES

- (1) Zewail, A. H.; Thomas, J. M. *4D Electron Microscopy: Imaging in Space and Time*; Imperial College Press: London, U.K., 2010.
- (2) Zewail, A. H. *Science* **2010**, *328*, 187.
- (3) Lorenz, U. J.; Zewail, A. H. *Proc. Natl. Acad. Sci. U.S.A.* **2013**, *110*, 2822.
- (4) Fitzpatrick, A. W. P.; Park, S. T.; Zewail, A. H. *Proc. Natl. Acad. Sci. U.S.A.* **2013**, *110*, 10976.
- (5) Zewail, A. H. *Sci. Am.* **2010**, *303*, 74.
- (6) Jiménez, J. L.; Nettleton, E. J.; Bouchard, M.; Robinson, C. V.; Dobson, C. M.; Saibil, H. R. *Proc. Natl. Acad. Sci. U.S.A.* **2002**, *99*, 9196.
- (7) Dubochet, J.; Adrian, M.; Chang, J. J.; Homo, J. C.; Lepault, J.; McDowell, A. W.; Schultz, P. Q. *Rev. Biophys.* **1988**, *21*, 129.
- (8) Fitzpatrick, A. W. P.; Debelouchina, G. T.; Bayro, M. J.; Clare, D. K.; Caporini, M. A.; Bajaj, V. S.; Jaroniec, C. P.; Wang, L.; Ladizhansky, V.; Müller, S. A.; MacPhee, C. E.; Waudby, C. A.; Mott, H. R.; De Simone, A.; Knowles, T. P.; Saibil, H. R.; Vendruscolo, M.; Orlova, E. V.; Griffin, R. G.; Dobson, C. M. *Proc. Natl. Acad. Sci. U.S.A.* **2013**, *110*, 5468.
- (9) Sunde, M.; Serpell, L. C.; Bartlam, M.; Fraser, P. E.; Pepys, M. B.; Blake, C. C. J. *Mol. Biol.* **1997**, *273*, 729.
- (10) Serpell, L. C.; Berriman, J.; Jakes, R.; Goedert, M.; Crowther, R. A. *Proc. Natl. Acad. Sci. U.S.A.* **2000**, *97*, 4897.
- (11) Schütz, A. K.; Soragni, A.; Hornemann, S.; Aguzzi, A.; Ernst, M.; Böckmann, A.; Meier, B. H. *Angew. Chem., Int. Ed.* **2011**, *50*, 5956.
- (12) Rizzo, T. R.; Park, Y. D.; Peteanu, L. A.; Levy, D. H. *J. Chem. Phys.* **1986**, *84*, 2534.

- (13) Morel, B.; Varel, L.; Conejero-Lara, F. *J. Phys. Chem. B* **2010**, *114*, 4010.
- (14) Knowles, T. P.; Fitzpatrick, A. W. P.; Meehan, S.; Mott, H. R.; Vendruscolo, M.; Dobson, C. M.; Welland, M. E. *Science* **2007**, *318*, 1900.
- (15) Mirsky, A. E.; Pauling, L. *Proc. Natl. Acad. Sci. U.S.A.* **1936**, *22*, 439.
- (16) Klotz, I. M. *Protein Sci.* **1993**, *2*, 1992.
- (17) Fersht, A. R.; Shi, J. P.; Knill-Jones, J.; Lowe, D. M.; Wilkinson, A. J.; Blow, D. M.; Brick, P.; Carter, P.; Waye, M. M. Y.; Winter, G. *Nature* **1985**, *314*, 235.
- (18) Sheu, S. Y.; Yang, D. Y.; Selzle, H. L.; Schlag, E. W. *Proc. Natl. Acad. Sci. U.S.A.* **2003**, *100*, 12683.
- (19) Henderson, R.; Baldwin, J. M.; Ceska, T. A.; Zemlin, F.; Beckman, E.; Downing, K. H. *J. Mol. Biol.* **1990**, *213*, 899.
- (20) Georgieva, D. G.; Kuil, M. E.; Oosterkamp, T. H.; Zandbergen, H. W.; Abrahams, J. P. *Acta Crystallogr.* **2007**, *D63*, 564.
- (21) Schotte, F.; Lim, M.; Jackson, T. A.; Smirnov, A. V.; Soman, J.; Olson, J. S.; Phillips, G. N., Jr.; Wulff, M.; Anfinsen, P. A. *Science* **2003**, *300*, 1944.